Science of the Total Environment 806 (2022) 150514

Contents lists available at ScienceDirect

Science of the Total Environment

journal homepage: www.elsevier.com/locate/scitotenv

Dynamics of organic matter molecular composition under aerobic decomposition and their response to the nitrogen addition in grassland soils

Qian Zhao [a], Allison M. Thompson [a], Stephen J. Callister [a], Malak M. Tfaily [a,b], Sheryl L. Bell [a], Sarah E. Hobbie [c], Kirsten S. Hofmockel [a,d,*]

[a] Earth and Biological Sciences Directorate, Pacific Northwest National Laboratory, Richland, WA, USA
[b] Department of Environmental Science, University of Arizona, Tucson, AZ, USA
[c] Department of Ecology, Evolution & Behavior, University of Minnesota, St. Paul, MN, USA
[d] Department of Agronomy, Iowa State University, Ames, IA, USA

HIGHLIGHTS

- The decomposition of labile compounds is regulated by mineral association.
- The metabolism of recalcitrant molecules is controlled by biochemical preservation.
- Molecular composition of the persistent carbon pool is consistent across ecosystems.
- N addition inhibits cumulative respiration and the convergence of SOM composition.

GRAPHICAL ABSTRACT

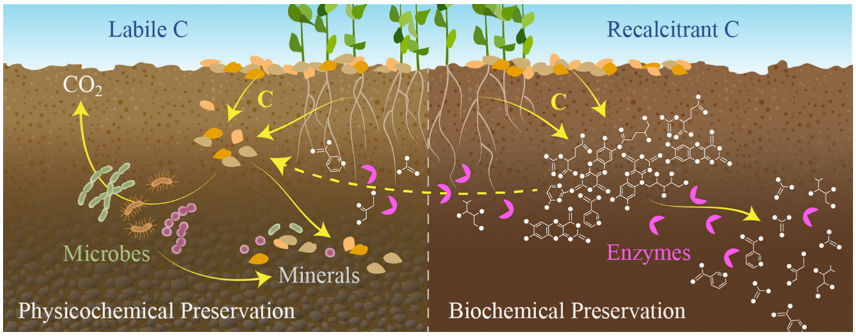

ARTICLE INFO

Article history:
Received 16 July 2021
Received in revised form 15 September 2021
Accepted 18 September 2021
Available online 22 September 2021

Editor: Jay Gan

Keywords:
Soil organic matter persistence
Mineral-organic matter association
Microbial decomposition
Respiration
Molecular transformation
Nitrogen fertilization

ABSTRACT

Grassland soils store a substantial proportion of the global soil carbon (C) stock. The transformation of C in grassland soils with respect to chemical composition and persistence strongly regulate the predicted terrestrial-atmosphere C flux in global C biogeochemical cycling models. In addition, increasing atmospheric nitrogen (N) deposition alters C chemistry in grassland soils. However, there remains controversy about the importance of mineralogical versus biochemical preservation of soil C, as well as uncertainty regarding how grassland soil C chemistry responds to elevated N. This study used grassland soils with diverse soil organic matter (SOM) chemistries in an 8-month aerobic incubation experiment to evaluate whether the chemical composition of SOM converged across sites over time, and how SOM persistence responded to the N addition. This study demonstrates that over the course of incubation, the richness of labile compounds decreased in soils with less ferrihydrite content, whereas labile compounds were more persistent in ferrihydrite rich soils. In contrast, we found that the richness of more complex compounds increased over the incubation in most sites, independent of soil mineralogy. Moreover, we demonstrate the extent to which the diverse chemical composition of SOM converged among sites in response to microbial decomposition. N fertilization decreased soil respiration and inhibited the convergence of molecular composition across ecosystems by altering N demand for microbial metabolism and chemical interactions between minerals and organic molecules. This study provides original evidence that the decomposition and metabolism of labile organic molecules were largely regulated by soil mineralogy (physicochemical preservation), while the metabolism of more complex organic molecules was controlled by substrate complexity

---

[*] Corresponding author at: Pacific Northwest National Laboratory, 902 Battelle Blvd, Richland, WA 99352, USA.
E-mail address: kirsten.hofmockel@pnnl.gov (K.S. Hofmockel).

https://doi.org/10.1016/j.scitotenv.2021.150514

(biochemical preservation) independent to mineral-organic interactions. This study advanced our understanding of the dynamic biogeochemical cycling of C by unveiling that N addition dampened C respiration and diminished the convergence of SOM chemistry across diverse grassland ecosystems.

1. Introduction

Grassland ecosystems are one of the largest terrestrial carbon (C) reservoirs, covering approximately one-third of the global terrestrial surface and storing ~20% of the global soil C stock (Conant et al., 2001; Scurlock and Hall, 1998). Increased atmospheric nitrogen (N) deposition caused by anthropogenic activities has a critical impact on ecosystem structure and function at the global scale, including on soil C cycling in grasslands (Bai et al., 2010; Gruber and Galloway, 2008). The decomposition and persistence of organic matter (OM) (see Table 1) in grassland soil and how they respond to elevated N inputs have the potential to significantly influence the global C cycle (Scurlock and Hall, 1998).

Decomposition of soil organic matter (SOM) is mainly mediated by microbial processes that rely on extracellular enzymes to break down organic polymers into oligomers and monomers (Garcia-Pausas and Paterson, 2011; Schimel and Schaeffer, 2012; Zhou et al., 2012a). 'Selective preservation' of SOM by microbial processes proposed that the labile C pool, including proteins, amino sugars, and carbohydrates of plant and microbial origin, is depleted over time (Feng et al., 2005). What remains is a suite of recalcitrant organic compounds, including lignin, tannin, and condensed aromatic C, that require more energy for microorganisms to decompose (Lehmann and Kleber, 2015; Lützow et al., 2006; Sollins et al., 1996). Such 'selective preservation' theory suggests that the microbial community regulates C decomposition, thus determining OM transformations in soil. In contrast, some studies demonstrated the decomposition of recalcitrant compounds could be more rapid than the decomposition of labile compounds as labile compounds could be associated with minerals to become chemically inaccessible from microbial decomposition (Klotzbücher et al., 2011; Lehmann and Kleber, 2015; Lützow et al., 2006).

The soil matrix plays a crucial role in the physicochemical persistence of SOM (Cotrufo et al., 2013; Six et al., 2002). Mineral-associated organic matter (MAOM) is a dominant form of relatively stable SOM, contributing up to 72% of total C in soils and sediments (Fang et al., 2019; Lalonde et al., 2012; Lehmann and Kleber, 2015; Lützow et al., 2006; Wagai and Mayer, 2007; Zhao et al., 2016). The multi-layer zonal structure model of mineral-OM complexes proposed that molecules enriched in hydrophilic C functional groups, fatty acids, and aromatic-rich molecules preferentially persisted to mineral surfaces, the hydrophobic zone, and the kinetic zone, respectively (Kleber et al., 2007). Our empirical study supports that protein- and lipid-like molecules preferentially accumulate in the hydrophobic zone and lignin-like molecules persist in the kinetic zone of the mineral-OM complexes from soil with more ferrihydrite content (Zhao et al., 2020). Thus, these molecular classes are inherently persistent because of their chemical interactions with mineral surfaces (Bahureksa et al., 2021; Kleber et al., 2007; Zhao et al., 2020).

Table 1
Glossary of key technical terms used in this paper.

Glossary	Description
Decomposition	A process of the breakdown of polymers into constituent oligomers, monomers.
Mineralization	A process that includes assimilation of molecules into microbial cells and transformations from organic to inorganic forms, including the respiration to CO_2.
Persistence	A condition of molecules that are resistant to microbial decomposition or molecules transformed during the incubation, but not assimilated or mineralized.
Recalcitrance	Chemical property of organic molecules based on molecular structure; a class of molecules with a high proportion of poly-condensed aromatic moieties are intrinsic molecular recalcitrance.
Short-range order/poorly crystalline mineral	The regular and predictable arrangement of atoms over a very short distance but not exceeding a few nanometers.

Elevated N inputs to soil has shown significant impacts on soil C decomposition and geochemical interactions (Chen et al., 2020; Huang et al., 2020a; Riggs et al., 2015; Zhang et al., 2014; Zhao et al., 2020). Previous studies found that experimental N addition has negative effects on the decomposition of SOM (Chen et al., 2020; Riggs et al., 2015; Tan et al., 2017). The decrease of SOM decomposition by N addition is likely caused by decreased lignin-degrading enzymes (Fog, 1988; Ramirez et al., 2012) and reduced microbial biomass (Lu et al., 2011; Treseder, 2008). Decreased C decomposition in response to N addition may not always result in the increase of soil C storage, given the large variation of soil C pools among different ecosystems. For instance, Lu et al. (2011) found that N addition resulted in minor changes in soil C storage from forest and grassland ecosystems, but a significant increase in agricultural soils because of relatively large, new C inputs from aboveground production in agricultural ecosystems. Moreover, N addition was found to increase the new C pool but have no impact or decrease old C in soil (Huang et al., 2020a; Hobbie et al., 2012). Thus, elevated N inputs have the potential to influence soil C storage depending on the SOM chemical composition. Meanwhile, previous studies have demonstrated that N addition decreased soil pH across multiple ecosystems (Chen et al., 2020; Riggs et al., 2015; Zhou et al., 2017; Zhao et al., 2020). N addition led to the accumulation of hydrogen ions (H^+) and nitrate (NO^{3-}) due to stimulated nitrification. Consequently, N addition-induced soil acidification potentially may decrease microbial decomposition by suppressing microbial growth (Rousk et al., 2009; Treseder, 2008) and altering microbial community composition (Rousk et al., 2010; Zhou et al., 2017). Soil acidification may also alter chemical interactions at the interface between minerals and OM (Yu et al., 2013; Zhao et al., 2020). Soils acidification resulted in more positive charges on both proteins and ferrihydrite surfaces (Yu et al., 2013), causing the loss of proteins because of disturbed electrostatic interactions. Soil acidification also causes the leaching of base cations (Ca^{2+} or Mg^{2+}) by disrupting cation bridging of OM on mineral surfaces (Rowley et al., 2018; Yu et al., 2017). Moreover, decreased pH increases the prevalence of ligand exchange on mineral surfaces by releasing H^+, resulting in more associations of OM (Kleber et al., 2005; Kögel-Knabner et al., 2008; Lützow et al., 2006). Therefore, N addition disrupted mineral-OM associations through altering chemical interactions, such as electrostatic interactions, H-bonds, and cation bridging (Bahureksa et al., 2021; Kleber et al., 2007; Zhao et al., 2020).

Building off these findings, a wide range of chemical composition of SOM from diverse grassland soils can persist by both chemical recalcitrance and mineral associations, resulting in a predictable pattern of C accumulation, by which grassland soils with high recalcitrant C content and/or short-range order minerals (also referred to as poorly crystalline minerals) accumulate more C. There is still a lack of information on a unifying mechanism of SOM persistence applicable across grassland ecosystems during microbial decomposition processes, and how the SOM persistence mechanism responds to the nutrient addition.

This study aims to test the extent to which the accumulation of molecules reflects persistence of compound classes due to chemical recalcitrance and mineral-OM associations. We hypothesized that in the absence of new C inputs, microbial decomposition of SOM will significantly decrease the richness of labile organic molecules that are bioavailable and vulnerable to decomposition, but increase the richness of organic compounds that are either chemically recalcitrant for microbial metabolism or inaccessible due to the association with minerals through depolymerization of recalcitrant compounds and sorption to mineral surfaces. In addition, we hypothesized that mechanisms for SOM persistence, by both chemical recalcitrance and mineral associations, are consistent across soils, resulting in a convergence of SOM chemistry across soils over the course of the incubation. Moreover, N fertilization will inhibit the molecular compositional convergence of SOM across soils during the incubation due to the reduction of microbial decomposition and the interference of organo-mineral associations. We expect that the reduced microbial decomposition will result from inhibited microbial growth and respiration induced by the N fertilization; meanwhile, the disrupted chemical interactions, such as electrostatic interactions, H-bonds, and cation bridging, in N-fertilized soils will interfere with the formation of organo-mineral associations.

2. Material and methods

2.1. Soil sampling and analysis

Soil samples were collected from six grassland sites (Table 2), which are a subset of grasslands from the Nutrient Network (NutNet) study (Borer et al., 2014), an ecosystem-scale nutrient addition field experiment spanning over 25 countries on five continents (Borer et al., 2014). This study explicitly focused on N-fertilized treatments at the NutNet field experiments to address the specific objective and hypothesis about the impact of increased N deposition on grassland soil chemistry and ecosystem functions as mentioned in the Introduction section. Each site included 3–6 replicated blocks. Each block had both N-fertilized and unfertilized plots (5 × 5 m). N-fertilized plots received 10 g N m^{-2} yr^{-1} timed-release urea, applied annually. Samples were collected in 2016 after eight years of field-experimental annual nutrient addition. Ten soil cores (1 cm diameter × 15 cm deep) were sampled from random locations in each plot and composited into a single sample. Surficial plant litter was removed from the top of each core and the three soil cores were homogenized to generate a composite plot sample. Soil was collected in pre-combusted foil packets and shipped to the lab on ice packs. In the lab, soils were 2 mm sieved at field moisture and visible roots that passed the sieve were removed. Soils were then stored at 4 °C. Soil characterization data, including soil field moisture, pH, and soil texture, were provided by Nutrient Network collaborators at https://nutnet.org/data. Field moisture was measured gravimetrically by subtracting weights before and after completely drying under 60 °C. Soil pH was determined in 1:1 soil:water suspension. Soil texture was determined by the pipette method on mass basis (Gee and Bauder, 1986). The total C and N concentrations of each soil sample were analyzed by a Vario EL Cube CHNS elemental analyzer from Elementar Americas, Inc. (Ronkonkoma, NY, USA). The amount of ferrihydrite (mmol/g soil) was calculated by multiplying the proportion of ferrihydrite in all Fe mineral phases with the total Fe content (wt %) of each soil (Zhao et al., 2020). We assume the Fe mineralogy did not change during the 8-month incubation.

2.2. Aerobic incubation

To target the mechanisms regulating SOM persistence, soils were incubated under aerobic conditions, in the absence of new C inputs, and wet-dry cycles were imposed to stimulate respiration of bioavailable C. This approach allowed us to reduce heterogeneity of soil C and investigate the contribution of physicochemical and biochemical mechanisms. Specifically, 25 g of soil at field moisture were added to a 125 mL glass incubation jar and placed in the incubator at a constant room temperature (20 °C) to avoid temperature variation effects on microbial activity. Soil samples were incubated with two successive weeks of wetting followed by one week of drying to maximize soil C respiration as wetting events increase diffusion and mobilize nutrients and organic substrates that accumulated during drought (Butterly et al., 2009; Tiemann and Billings, 2011). The total incubation lasted 224 days (CP samples were incubated for 203 days due to the late sampling date). Soils were wet to their field moisture on the first day of wet weeks using sterilized HPLC analytical grade H_2O. Jars were tightly capped with lids for the first 24 h of each week to capture respired CO_2. For the rest of time, lids without septa (open to ambient air) were placed on jars for the aerobic incubation. The CO_2 concentration in the headspace was measured after the 24 h-capped period by an infrared gas analyzer on a LI-7000 (Licor, Lincoln, NE, USA). Gas samples were obtained through septa of tightly capped jar lids via a syringe with a needle. Cumulative C was calculated by using the CO_2-C respired in the first 24 h after weekly rewetting events, and we assumed that limited C respiration occurred for the rest of each week after 24 h of the wetting event. Given the limited amount of soil from field and the confounding factors associated with the sterilization of soil, this study did not include abiotic controls in the incubation experiment. Soils were subsampled for subsequent analyses at the initial (T_i) and final (T_f) time points corresponding to the beginning (immediately after incubations were established) and end of the 8-month incubation. Microbial biomass subsamples from T_i and T_f were kept at field moisture

Table 2
Characteristics of six unfertilized and N-fertilized study sites, located in the Central and Intermountain Western USA.

Site or soil characteristic	Lookout ridge, OR (n = 3)		Cedar creek LTER, MN (n = 5)		Bunchgrass, OR (n = 3)		Shortgrass steppe LTER, CO (n = 3)		Cedar point biological station, NE (n = 6)		Sevilleta LTER, NM (n = 4)	
Site abb.	LK		CC		BG		SG		CP		SV	
Habitat	Montane grassland		Tallgrass prairie		Montane grassland		Shortgrass prairie		Shortgrass prairie		Desert grassland	
Soil Order	Andisols		Entisols		Inceptisoles		Entisols		Mollisols		Aridisols	
MAP (mm)	898		50		647		65		45		52	
MAT (°C)	4.8		6.3		5.5		8.4		9.5		12.6	
Moisture (%)	37.6		6.6		24.6		9.2		3.2		4.1	
Clay (%)	0.8		2.5		2.9		8.8		9.8		5.6	
Silt (%)	30.1		8.1		26.5		17.1		19.9		9.9	
Sand (%)	69.0		89.3		70.4		74.0		70.2		84.4	
Ferrihydrite (mmol/g soil)	0.53		0.06		0.44		0		0		0.07	
Treatment	Unfer	N-fer	Unfer	N-fer	Unfer	N-fer	Unfer	N-fer	Unfer	N-fer	Unfer	N-fer
pH	4.9	4.7	6.1	5.6	5.7	5.1	6.6	6.3	7.2	6.4	8.4	8.3
Total C (%)	18.63	14.50	0.58	1.11	7.86	8.97	0.76	0.81	1.10	1.23	0.34	0.31
Total N (%)	1.26	1.04	0.043	0.076	0.55	0.62	0.078	0.085	0.097	0.11	0.03	0.032
C/N	14.74	13.94	13.52	14.67	14.43	14.39	9.75	9.54	11.42	11.40	11.02	9.48

MAP, mean annual precipitation; MAT, mean annual temperature; LTER, Long Term Ecological Research; Unfer: unfertilized soil; N-fer: N-fertilized soil; soil pH, moisture, and texture from Nutrient Network collaborators.

and measured within 24 h. Both T_i and T_f subsamples were air-dried and stored for C chemical characterizations, such as C and N concentrations and high-resolution mass spectrometry described below.

2.3. Microbial biomass carbon

A sequential chloroform ($CHCl_3$) fumigation direct extraction method modified from Witt et al. (2000) was used to measure microbial biomass C and salt-extractable C contents. Briefly, 8 g of soil was weighed in a 50 mL falcon tube and mixed with 24 mL of 0.5 M K_2SO_4. Samples were shaken at 200 rpm at 20 °C for 2 h. The soil slurry was centrifuged, and the supernatant was filtered through pre-leached 2.5 μm filter paper (Whatman grade 42). Then, the soil pellet and the filter from the initial extraction were mixed with 2 mL of $CHCl_3$ directly and fumigated for 48 h. Fumigated samples were re-extracted with 24 mL of 0.5 M K_2SO_4. Shaking, centrifugation, and filtration were repeated with the same conditions as the initial extraction. Microbial biomass C content was determined by the salt-extractable C content of the fumigated extract minus the salt-extractable C content from the unfumigated extract, quantified by a Vario TOC Cube analyzer (Elementar, Germany).

2.4. Carbon chemistry analysis

Water (H_2O) and a mixture of methanol (MeOH) and $CHCl_3$ were sequentially used to extract organic molecules from T_i and T_f soil samples for chemical characterization using Fourier transform ion cyclotron resonance mass spectrometry (FTICR-MS) (Tfaily et al., 2015, 2017). Briefly, 300 mg of soil sample was mixed with 1 mL of HPLC analytical grade H_2O and shaken for 2 h on an Eppendorf Thermomixer in 2 mL capped glass vials. Water extraction releases labile and polar organic molecules that represent water extraction organic carbon (WEOC). The soil pellet was then mixed with a mixture of $CHCl_3$ and MeOH in a 2:1 ratio and shaken for 2 h. The upper layer contains the MeOH extracts, which have overlapping compounds with WEOC and was not included in this study. The lower layer contains the lipid-like, hydrophobic molecules from the $CHCl_3$ extraction. Ultrahigh resolution characterization of SOM in the H_2O and $CHCl_3$ extracts was carried out using a 12 Tesla Bruker SolariX FTICR mass spectrometer, respectively. The FTICR-MS data from H_2O and $CHCl_3$ extracts were then composited for further data analyses to represent OM from the dynamic pool (WEOC + hydrophobic fraction). The dynamic pool of SOM was operationally defined to target organic molecules that can be accessed by soil microbes, including the kinetic and hydrophobic zones in the multi-layer zonal structure model of mineral-OM complexes (Kleber et al., 2007; Zhao et al., 2020). Although we acknowledge that other solvents (dithionite, HCl-hydroxylamine, ammonium oxalate, and sodium pyrophosphate) can target a greater portion of the SOM pool (Coward et al., 2017; Heckman et al., 2018), this study focuses on microbial decomposition processes of SOM and therefore characterized the chemical dynamics of organic molecules that likely were accessible to microbial decomposition. Samples from LK site were not included in the FTICR-MS results because of an issue during the ionization of FTICR-MS analysis with a dominating silica-containing peak, which should not be present in our samples in such high abundance.

2.5. Molecular composition and transformation analysis

To aid in the interpretation of FTICR-MS data, the chemical characteristics of thousands of organic molecules were evaluated by plotting the van Krevelen diagram on the basis of their molar H:C ratios (y-axis) and molar O:C ratios (x-axis). Chemical classes, including amino sugar, protein, lipid, carbohydrate, unsaturated hydrocarbon, condensed hydrocarbon, lignin, and tannin, can be assigned to molecular compounds based on their O:C and H:C ratios (Supplementary Table S1) (Kim et al., 2003). To decrease the molecular complexity, the labile C compounds include amino sugar-, protein-, lipid-, carbohydrate-, and unsaturated hydrocarbon-like molecules, which can be rapidly decomposed and mineralized with relative low energy (Feng et al., 2005; LaRowe and Van Cappellen, 2011). The recalcitrant C compounds include condensed hydrocarbon-, lignin-, and tannin-like molecules, which have a greater prevalence of polycondensed aromatic moieties and can be slowly decomposed, compared with labile C (Kleber, 2010; Lehmann and Kleber, 2015; Lützow et al., 2006; Sollins et al., 1996). The richness of compounds represents the number of molecules present in a given sample. To present only those compounds that were identified by FTICR-MS analysis with high accuracy, the richness of compounds was calculated from the compounds that were present in over 50% of replicates from the same treatment. The compounds richness was then normalized by the C content of the dynamic C pool, expressed as # of molecules/mg C. Changes in the normalized compound richness present between T_i and T_f were expressed as either absolute values, (# of molecules/mg C at T_f) − (# of molecules/mg C at T_i) or log 2-fold change, $\log_2(T_f/T_i)$. Positive values represent more compounds in T_f, signifying depolymerization, while negative values represent more compounds in T_i, signifying microbial assimilation and/or loss via respiration.

The mass differences between any two FTICR–MS peaks within each sample were determined to identify putative molecular transformations that indicate potential decomposition pathways of SOM. For instance, a mass difference of 2.0156 Da indicates a hydrogenation/dehydrogenation reaction; and a mass difference of 57.0215 Da represents a reaction involving a loss or gain of glycine. The downstream analysis used a subset of all mass differences that correspond to commonly observed biochemical transformations adopted from Breitling et al. (2006). The total count of all putative molecular transformations was determined by the number of times all transformations were observed within each sample. To contrast potential decomposition pathways of SOM across sites, incubation times, and fertilization treatments, the total count of molecular transformations was compared between sites, times, and treatments. To further account for the chemical classes of compounds in which each transformation was involved, all putative molecular transformations within each sample were grouped by the chemical classes of two peaks that were used to determine the mass differences. The counts of putative molecular transformations for compounds from each chemical class can potentially represent the metabolic activities of microorganisms that decompose compounds from different chemical classes.

2.6. Data analysis/statistics

The correlation between the total cumulative C respired at T_f and soil chemical properties was analyzed by Pearson correlation. Two-way analysis of variance (ANOVA) was used to assess the effects of fertilization treatment and site on the total cumulative C respired at T_f. As ANOVA found non-significant interaction and main effect of treatment on the total cumulative C respired and non-independence between site and treatment (χ^2 (23) = 93.9, $p < 0.001$), linear mixed-effects models (LMM) were then conducted to determine the fertilization treatment effect on repeated measures of cumulative C and respiration rate while controlling for the site effect. In the LMM, site, block, and incubation time (weekly time points) were fitted as random effects, with incubation time nested within block and block nested within site. This model fitting accounted for potential spatial and temporal autocorrelation by considering the finer-scale variables nested within the broader-scale variables. Treatment (N-fertilized vs. unfertilized) was considered as a fixed effect in the LMM. The LMM was fit in the 'lme4' package in R (version 4.0.0) using the 'lmer' function. Liner regression was conducted to determine how changes in the normalized richness of compounds was associated with soil mineralogy and texture. Chemical composition similarity between the two time points (T_i and T_f) was computed by

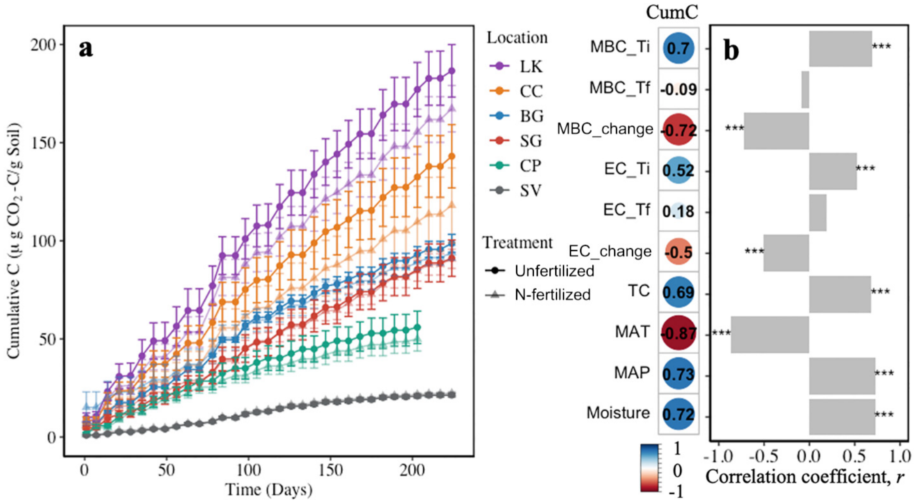

Legend:
MBC – microbial biomass carbon, EC – salt-extractable carbon, TC – total carbon,
MAT – mean annual temperature, MAP – mean annual precipitation,
MBC_change or EC_change - changes in MBC or EC (Tf - Ti)

Fig. 1. a) Cumulative C respired as CO_2 for six unfertilized and N-fertilized soils during 224-day aerobic incubation, b) correlations between cumulative C respired and soil properties from both unfertilized and N-fertilized soils. The size and color of circles and bars indicate Pearson correlation coefficients, r. $^{***}p < 0.001$.

Jaccard dissimilarity matrices of presence/absence FTICR-MS data. The effect of time on the chemical composition similarity was tested by using permutational multivariate ANOVA (PERMANOVA) implemented in the 'adonis' function in the 'vegan' package in R (Version 4.0.0) and visualized using Non-metric Multidimensional Scaling (NMDS, 'vegan'). Statistical analyses were conducted using R software (https://www.r-project.org). All effects were considered significant at $p < 0.05$ unless noted.

3. Results

3.1. SOM mineralization

Over the 8-month aerobic incubation, across six unfertilized grassland sites, the average C loss through cumulative respiration ranged from 21.4–186.6 μg CO_2-C/g soil (Fig. 1a), accounting for 0.1–2.48% of total soil C. Andisols from LK had the highest cumulative C respired, whereas aridisols from SV had the lowest among all sites. Cumulative C respired per gram soil was positively correlated with mean annual precipitation (MAP) ($r = 0.73$, $p < 0.001$), soil moisture ($r = 0.73$, $p < 0.001$), initial (field) microbial biomass C ($r = 0.70$, $p < 0.001$) and salt-extractable C ($r = 0.52$, $p < 0.001$); however, cumulative C was negatively correlated with mean annual temperature ($r = -0.87$, $p < 0.001$), changes in microbial biomass C (T_f-T_i) ($r = -0.72$, $p < 0.001$) and salt-extractable C ($r = -0.50$, $p < 0.001$) (Fig. 1b). Cumulative C in CO_2 did not plateau by the end of the 8-month incubation with final respiration rates of 1.45–5.18 μg CO_2-C/g/d for unfertilized soil from five out of six sites (except SV) (Fig. S1). Cumulative C plateaued in SV with the final respiration rate of 0.08 μg CO_2-C/g/d, likely because of its low C content. The total cumulative C respired from unfertilized soils differed significantly among sites (ANOVA, $p < 0.001$) (Fig. 1a), reflecting differences in the mineralizable C pool (e.g., microbial biomass C or salt-extractable C) across sites (Table 3). Moreover, the three sites with the most cumulative C respired had decreased microbial biomass C over the course of the incubation, of which the two Oregon sites (LK and BG) had greater decreases in microbial biomass C compared to cumulative C respired, whereas the sites with lower soil respiration increased in microbial biomass C (Fig. 1b and Table 3).

N fertilization significantly decreased the average C respiration rates (by 0.264 μg CO_2-C/g/d) and cumulative C respired (by 4.97 μg CO_2-C/g) across six grassland sites over the 8-month incubation, compared with unfertilized soils (Fig. 1a and S1, LMM, $p < 0.001$ for both). However, N fertilization enhanced the total cumulative C respired by 4.1% on the aridisols (SV), which had the lowest C content (Fig. 1a).

Table 3
Microbial biomass C and salt-extractable C contents of six study sites.

Treatment	Sites	Microbial biomass C (μg/g soil)				Salt-extractable C (μg/g soil)			
		T_i	T_f	changes (T_f-T_i)	log2 FC[a]	T_i	T_f	changes (T_f-T_i)	log2 FC
Unfertilized soil	LK (n = 3)	959.4	70.9	−888.5	−3.8	429.6	101.4	−328.2	−2.1
	CC (n = 5)	170.3	133.5	−36.8	−0.4	21.5	57.3	35.8	1.4
	BG (n = 3)	706.0	306.0	−399.9	−1.2	289.9	240.4	−49.5	−0.3
	SG (n = 3)	72.9	84.0	11.1	0.2	21.5	22.6	1.2	0.1
	CP (n = 6)	22.4	209.5	187.2	3.2	33.2	69.1	35.9	1.1
	SV (n = 4)	46.5	88.0	41.5	0.9	36.9	32.4	−4.4	−0.2
N-fertilized soil	LK (n = 3)	903.0	69.0	−833.9	−3.7	462.9	78.7	−384.2	−2.6
	CC (n = 5)	148.3	103.2	−45.1	−0.5	54.0	94.2	40.2	0.8
	BG (n = 3)	696.6	292.3	−404.3	−1.3	462.3	243.9	−218.5	−0.9
	SG (n = 3)	67.9	95.5	27.6	0.5	259.0	61.3	−197.7	−2.1
	CP (n = 6)	18.9	194.8	175.8	3.4	25.7	117.3	91.7	2.2
	SV (n = 4)	47.9	62.3	14.4	0.4	50.5	37.8	−12.7	−0.4

Note: a. log2FC refers to log2 fold change. Values in this table are means of replicates.

3.2. Richness of organic molecules

High-resolution mass spectrometry-informed chemical characterization of SOM highlighted the diversity of organic molecules in the dynamic C pool across grassland sites. A total of 49,229 organic molecules were identified from the dynamic C pool of five unfertilized and N-fertilized grassland soils. The richness of organic compounds ranged from 4520 to 19,146 with BG (inceptisols) and CP (mollisols) sites containing the highest number of molecules and CC (entisols) having the least. Chemical classes revealed that lipid-like and lignin-like molecules dominated the dynamic pool of most grassland soils (Fig. S2). Regardless of incubation times and treatments, the richness of lignin-like molecules contributed 25.8 ± 8.6% (mean ± standard deviation) of the overall richness of organic molecules from the dynamic C pool across five soils, followed by lipids (19.6 ± 4.4%) and condensed hydrocarbons (8.8 ± 2.0%) (Fig. S2).

Over the course of the incubation, microbial decomposition of SOM decreased the normalized richness of labile compounds (lipid-, protein-, amino sugar-, carbohydrate, and unsaturated hydrocarbon-like) in three out of five unfertilized soils (except BG and SV) but significantly increased the normalized richness of recalcitrant compounds, such as condensed hydrocarbon-, tannin-, and lignin derivatives-like compounds in most unfertilized soils (Fig. 2a, b, and S3). A higher richness of labile compounds was found at T_i than that at T_f in entisols (CC, SG) and mollisols (CP), normalized by carbon content (Fig. 2a). For instance, in CP, soil at T_i had 20 times more labile compounds by a factor of 2 than soil at T_f. However, inceptisols (BG) and aridisols (SV) had a higher normalized richness of labile compounds at T_f than T_i, in contrast to the other sites (Fig. 2a). In addition, a higher normalized richness of recalcitrant compounds was present at T_f compared to T_i across most unfertilized soils (except CP) (Fig. 2b), indicating the accumulation of recalcitrant decomposition products that were resistant to decomposition, compared with other compounds that were mineralized during the incubation.

Changes in the normalized richness of labile and recalcitrant compounds over the course of the incubation were similar in N-fertilized and in unfertilized soils (Fig. 2a, b vs. Fig. 2c, d). The normalized richness of labile compounds decreased over the course of incubation in three out of five N-fertilized soils (except BG and SV), whereas the normalized richness of recalcitrant compounds increased over time in most N-fertilized soils (no changes in CP) (Fig. 2c, d).

The site-dependent changes in labile compound richness over the course of incubation were related to soil mineralogy. In particular, changes in the normalized richness of labile compounds ($T_f - T_i$) were positively correlated ($R^2 = 0.42$) with the amount of ferrihydrite across five soils, including both unfertilized and N-fertilized sites (Fig. 2e). Although inceptisols (BG) had higher amounts of ferrihydrite than the other sites, the correlation between changes in the normalized richness of labile compounds ($T_f - T_i$) and the amount of ferrihydrite remained significantly positive even when samples from BG site were removed from the statistical test ($p = 0.05$; $R^2 = 0.62$, Fig. S4). However, changes in the normalized richness of recalcitrant compounds ($T_f - T_i$) were not correlated with the amount of ferrihydrite (Fig. 2f), indicating soil Fe mineralogy did not drive site variations in time-

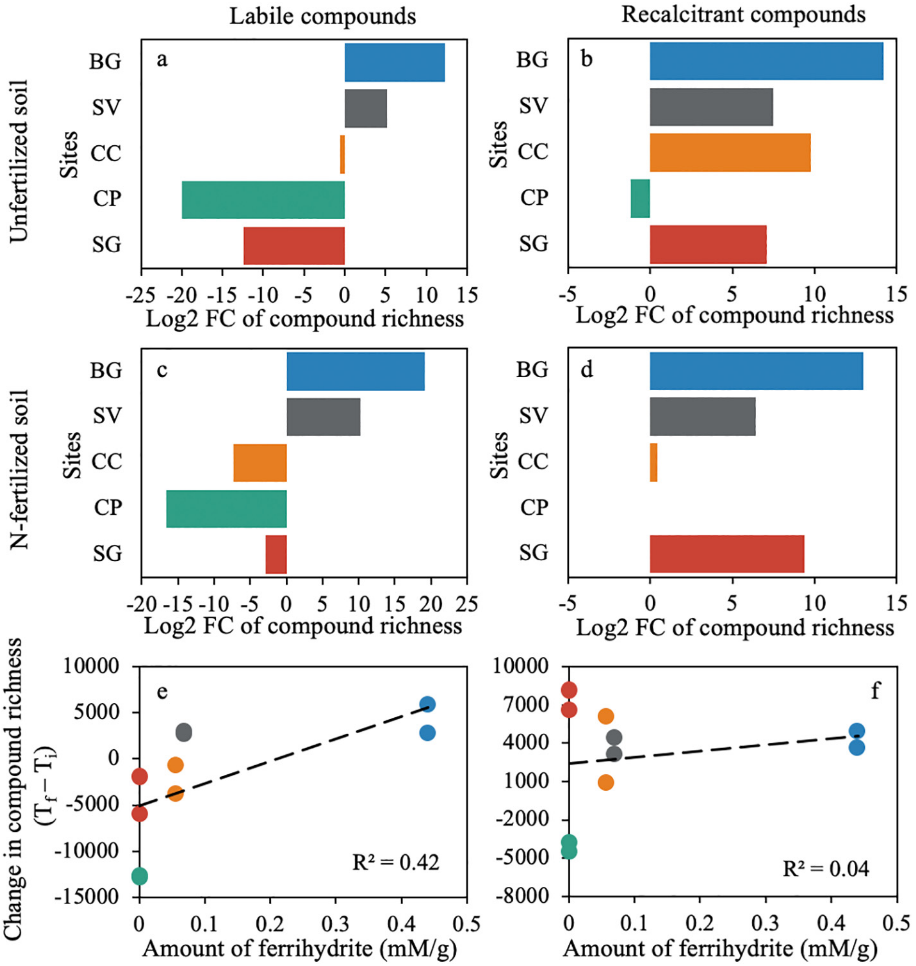

Fig. 2. Differences in the normalized compound richness present between T_i and T_f, expressed as $\log_2(T_f/T_i)$, from five unfertilized (a–b) and N-fertilized (c–d) soils. Panels a, c, and e show labile compounds, while panels b, d, and f show recalcitrant compounds. Positive values represent more compounds in T_f, while negative values represent more compounds in T_i. e and f: correlations between changes in normalized compound richness ($T_f - T_i$) and the amount of ferrihydrite across soils from both five unfertilized and N-fertilized sites.

evolved recalcitrant compound richness. Moreover, organic compounds may associate with minerals not only through poorly crystalline structure of minerals, but also via the small particle size of minerals in soil. Surprisingly, we found a significant negative correlation between changes in normalized richness of labile compounds and the content of clay size particles ($R^2 = 0.54$, Fig. S5) but no significant correlation with changes in the normalized richness of more complex compounds. This result suggests that for the soils in this study small particle size does not promote the persistence of labile compounds, but instead properties of ferrihydrite do. Ferrihydrite is characterized by not only the nanoscale particle size and large surface area, but also the prevalence of hydroxyl groups on the surface. Thus, chemical interactions between labile compounds with acidic organic ligands and hydroxyl groups at the ferrihydrite surface (Kaiser and Guggenberger, 2000) likely led to the accumulation of labile compounds in soils with more ferrihydrite content.

3.3. Dynamics of chemical composition

The chemical composition of organic molecules in the dynamic C pool was altered significantly by microbial decomposition. The binary NMDS plot representing the Jaccard dissimilarity of chemical compositions between samples shows a significant time effect for unfertilized soils ($F(1,n) = 4.58$, $p = 0.001$, Fig. 3a) and N-fertilized soils ($F(1,n) = 2.41$, $p = 0.019$, Fig. 3b). These shifts in chemical composition are supported by changes in the normalized richness of labile and recalcitrant compounds within the dynamic C pool (Fig. 2).

The composition of organic molecules from the dynamic C pool was more consistent across five unfertilized soils at T_f, compared with that at T_i (Fig. 3a). Visually, we observed that the chemical composition at T_f clustered more tightly than T_i in unfertilized soil, suggesting a greater similarity in the chemical composition among sites at T_f, compared to that at T_i (Fig. 3a). To statistically test the convergence of the chemical composition of organic molecules, the pairwise distance between individual samples at the beginning and end of the incubation was tested. The median pairwise distance decreased significantly over the aerobic decomposition in unfertilized soils (ANOVA, $p = 0.033$, Fig. 3c). The decreased median pairwise distance in Jaccard dissimilarity over time indicates more similar compound compositions between samples from five unfertilized soils at the end compared to the beginning of the incubation. In contrast, the median pairwise distance between samples from the two time points of N-fertilized soils were comparable, with no statistically significant difference (ANOVA, $p = 0.608$).

3.4. Molecular transformation

Significant differences in the counts of molecular transformations suggests different metabolic activities among grassland sites, times, and treatments. The total transformation counts were significantly different across five sites (ANOVA, $p < 0.001$), in which inceptisols (BG) and mollisols (CP) had relatively higher transformation counts than the other three sites (Fig. 4a), indicating potentially high metabolic activities in these two sites. By grouping molecular transformations into each chemical class, significant differences in transformation counts across sites were found in amino sugar ($p < 0.001$), carbohydrate ($p < 0.001$), condensed hydrocarbon ($p < 0.001$), lignin ($p < 0.001$), protein ($p = 0.001$), and tannin ($p < 0.001$) chemical classes (Fig. S6). The total count of molecular transformations significantly increased after the incubation ($p = 0.017$, Fig. 4b). Molecular transformations of condensed hydrocarbon- ($p < 0.001$) and tannin-like ($p < 0.001$) compounds were upregulated after the incubation (Fig. 4e), indicating that recalcitrant compounds were actively transformed during the incubation, but not assimilated or mineralized. This result supports the increased normalized richness of recalcitrant compounds as decomposition products in most soils (Fig. 2b and d).

4. Discussion

4.1. Shift in molecular composition

Decomposition changed the normalized richness of organic compounds reflecting different biogeochemical pathways of labile and

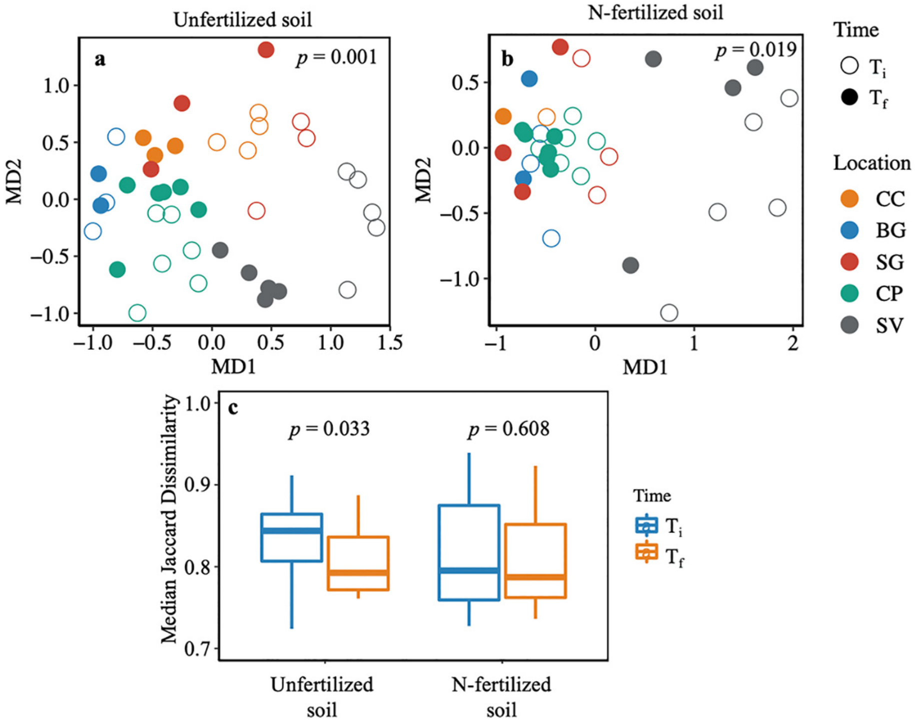

Fig. 3. NMDS plot of chemical compositions of organic molecules in the dynamic C pool at T_i and T_f for a) unfertilized and b) N-fertilized soils; c) dissimilarity of chemical compositions from five sites for T_i and T_f. Statistical significance in panel a and b was determined for PERMANOVA comparing the Jaccard dissimilarity between samples from two times; statistical significance in panel c was done by ANOVA comparing the median of pairwise distance between two times for data in above NMDS plots.

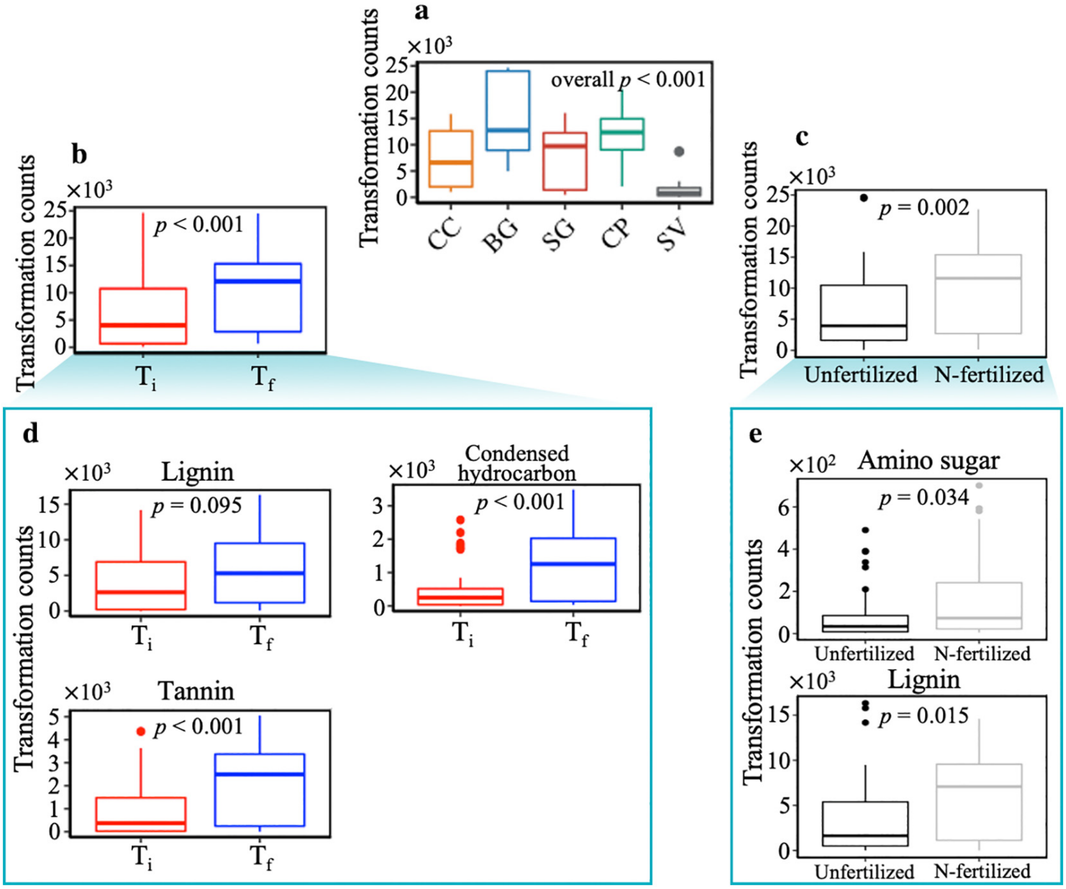

Fig. 4. Putative molecular transformation counts across a) grassland sites, b) incubation time, and c) fertilization treatment; d) molecular transformation counts in chemical classes with significant time effect; and e) molecular transformation counts in chemical classes with significant treatment effect. Putative molecular transformations were determined as the mass differences between any two FTICR–MS peaks within each sample (see Method, Section 2.5).

recalcitrant compounds. The richness of labile organic compounds declined at some sites, suggesting these compounds were mineralized by microbial activities. However, in sites with high poorly crystalline Fe oxide content, richness of labile compounds increased, perhaps because of stabilization of these compounds and their decomposition products on to minerals. Microbial decomposition preferentially mineralizes easily decomposable C sources that are accessible by microorganisms (Van Gestel et al., 1993). The depletion of labile (respired) C in this study was regulated by field soil moisture with soils collected from wetter sites exhibiting greater cumulative C respiration in the incubation experiment (Fig. 1). The microbial activity for organic C metabolism is primarily controlled by moisture, and water pulses from periodic precipitation in grassland soils can increase microbial resource availability because of the altered osmotic potentials of cells and increased diffusion (Austin et al., 2004; Schimel, 2018; Tiemann and Billings, 2011). Thus, wetting events during the incubation likely stimulated the release of intracellular labile C and mobilized nutrient sources to enhance microbial activity and support respiration (Austin et al., 2004; Halverson et al., 2000). Our results indicated that soil with higher field moisture had higher initial microbial biomass C (Fig. 1b, Table 3) to support C metabolism. In addition, soils with more cumulative C respired had decreased microbial biomass C over the course of the incubation. Microorganisms at these sites were limited by C resources during the incubation without new C inputs, resulting in a tradeoff between C allocation to respiration and to microbial production. Microbial biomass turnover exceeded cumulative respiration in two Oregon sites, suggesting that microbial necromass was accumulating and likely persisting due to mineral associations. Previous studies found that proteins preferentially persist through sorption to ferrihydrite surfaces (Kleber et al., 2007; Yu et al., 2013; Zhao et al., 2020). These two sites have the most ferrihydrite content among all sites according to results from our previous study (Zhao et al., 2020). Meanwhile, the other three sites with lower soil respiration increased their microbial biomass C during the incubation (Fig. 1b and Table 3). The dynamics of biomass C discussed here also support the changes in labile compound richness during the incubation. We found that soils with high ferrihydrite content had increases in their normalized richness of labile compounds (Fig. 2e), which include proteins- and amino sugar-like molecules that are important constituents of necromass.

The highly diverse grassland microbiome is capable of decomposing not only labile but also recalcitrant compounds. The presence of O_2 removed the thermodynamic constraint for the microbial decomposition of SOM, given that O_2 was being used as the terminal electron acceptor under aerobic condition. The decomposition of recalcitrant organic compounds requires multiple steps: depolymerization, aromatic ring cleavage, and mineralization (Datta et al., 2017). The increased normalized richness of recalcitrant compounds in most soils (Fig. 2b and d) is likely caused by the depolymerization process, which generates new oligomers (Fig. 5). Relatively high molecular weight recalcitrant compounds were broken down to a variety of relatively low molecular weight compounds by enzymes (Fig. S7). The newly generated decomposition products and cell walls from turnover of biomass that contains recalcitrant compounds resulted in the increased richness of recalcitrant compounds. The molecular transformation counts reflect the active metabolic pathways. After the 8-month incubation, soils had higher transformation counts that at initiation of the incubation, suggesting that more organic compounds, including both labile and recalcitrant compounds, were decomposed or transformed via metabolic pathways during the incubation. Overall, the shifted chemical composition of SOM fully supports the first hypothesis, by which some labile compound classes were

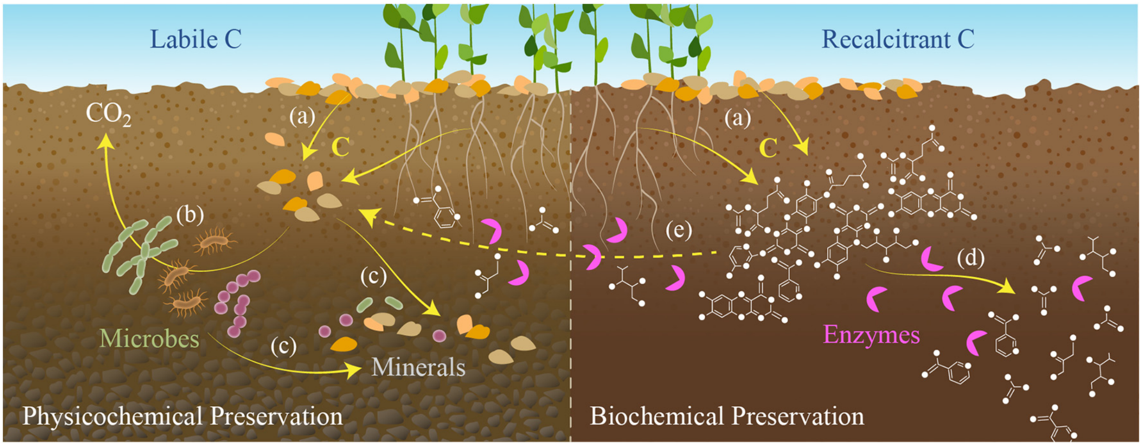

Fig. 5. Conceptual model of the dynamics of labile and recalcitrant C pools during microbial decomposition. a) Highly diverse organic molecules grouped as labile and recalcitrant C pools contribute to grassland soil from plant derivates, root exudates, and microbial biomass. b) Labile C compounds can be rapidly decomposed and mineralized by microbes with relative low energy. c) Soil minerals adsorb and persist labile compounds and microbial biomass/necromass. d) Recalcitrant C compounds can be decomposed via depolymerization and aromatic ring cleavage. e) The depolymerization of recalcitrant C compounds generates labile molecules.

depleted in richness, at least at some sites, while recalcitrant compounds were transformed and accumulated over the course of the incubation at most sites.

4.2. Consistent molecular composition of the persistent C pool across ecosystems

The chemical composition of organic compounds after microbial decomposition was similar across sites suggesting consistent biochemical and physicochemical C stabilization mechanisms, reflecting the importance of OM functional group interactions with soil minerals. The highly diverse chemistry of SOM across ecosystems reflects heterogeneous molecules from two dominant sources: plant derivates and microbial biomass (Angst et al., 2021). Microbial communities and plant communities have shown significant differences across NutNet sites (Leff et al., 2015). However, in support of our hypothesis, the increased similarity of SOM chemistry among ecosystems following decomposition without new C inputs suggests consistent mechanisms for SOM persistence across grassland soils.

The physicochemical persistence of SOM by organo-mineral interactions has been well documented (Kleber et al., 2015; Lavallee et al., 2020; Schmidt et al., 2011; Torn et al., 1997; Zhao et al., 2020). Fe-bearing minerals have been found to effectively preserve SOM, stabilizing 3–72% of total organic C in soil and sediment across different ecosystems, including in grasslands (Fang et al., 2019; Kramer and Chadwick, 2018; Lalonde et al., 2012; Wagai and Mayer, 2007; Zhao et al., 2016). Short-range order Fe oxides preferentially sorb hydrophilic molecules, such as proteins or hydrophilic fractions of lipids, via electrostatic interactions (Kleber et al., 2007; Zhao et al., 2020). Ferrihydrite, a poorly crystalline Fe oxide, is predominant in inceptisols (BG) and aridisols (SV) (Zhao et al., 2020), which showed a stronger preservation of labile compounds, including proteins, carbohydrates, and amino sugars during microbial decomposition, compared with other sites (Fig. 2 and S3). The positive correlation between the increase of labile compound richness and ferrihydrite content suggests the critical role of minerals stabilizing easily decomposable C, thus regulating SOM chemical composition in grassland ecosystems.

Biochemical mechanisms of C persistence could also strongly regulate the accumulation of C in grassland ecosystems. The decomposition of recalcitrant compounds (i.e., lignin, tannin, condensed hydrocarbons) is typically driven by fungi and actinobacteria that produce oxidative enzymes, such as lignin peroxidases, to break down organic polymers into oligomers and monomers (Schimel and Schaeffer, 2012; Sinsabaugh, 2010). However, such biotic decomposition typically occurs over a long period of time because relatively few microbes have oxidative capability and their reactions slow under certain environment, such as anaerobic conditions (Janusz et al., 2017; Thevenot et al., 2010). Alternatively, the decomposition of recalcitrant compounds could also be initiated abiotically. Strong oxidants, such as hydroxyl radicals, are needed to initiate non-enzymatic attack of recalcitrant compounds, such as molecules from plant cell walls (Goodell, 2003; Hall and Silver, 2013; Halliwell and Gutteridge, 2015; Huang et al., 2020b). Although hydroxyl radicals are present in biological systems, they are in low abundance due to their short half-life in natural environments. This is why recalcitrant compounds are slowly decomposed, and biochemical preservation is more pronounced for these compounds, compared with labile compounds.

Collectively, this study provides original evidence that the decomposition and metabolism of labile organic molecules were largely regulated by soil mineralogy while the metabolism of more complex organic molecules was controlled by substrate complexity rather than mineral-organic interactions. The biochemical complexity of organic molecules primarily constrains the decomposition of soil C, independent of soil mineralogy. Subsequently, the decomposition of labile compounds that are not energetically constrained due to recalcitrance (biochemical preservation), was dependent on the ferrihydrite content in soil (physicochemical preservation) (Fig. 3e, f). Therefore, consistent contributions of both physicochemical and biochemical preservation of SOM result in similar composition of molecules resisting microbial decomposition across ecosystems.

4.3. Inhibition in cumulative C and molecular composition shift by the N addition

Long-term N addition showed an inhibition of C decomposition, as indicated by the retarded cumulative C respired over the course of incubation (Fig. 1). Negative responses of soil respiration to N addition in grassland soils have been found in other studies (Ramirez et al., 2010; Riggs et al., 2015; Zhang et al., 2014). Uptake and assimilation of N are energy-consuming processes (Engels and Marschner, 1995). When soil is supplemented with N, microbes may spend less energy on N acquisition, e.g., from decomposition of SOM, compared with unfertilized soil (Zhou et al., 2012b). In addition, decreased microbial biomass C with N addition in the present study (Table 3) suggests that reduced microbial growth and biomass production may potentially reflect the limited C availability for microbial assimilation due to altered microbial community and enzyme activities by N addition (Ramirez et al., 2012). Chronic N addition may facilitate C leaching out of grassland ecosystem by soil acidification, thereby decreasing bioavailable C for microbial growth (Evans et al., 2008; Liu and Greaver, 2010). Thus, N addition-induced decreases in C availability, microbial growth, and biomass production have led to decreased SOM decomposition and respiration in grassland soil, in line with a previous meta-analysis study of multiple field studies by Treseder (2008).

In this study, we have evidence that fully supports the last hypothesis. N addition inhibited C decomposition not only by decreasing respiration and microbial biomass, but also by altering chemical interactions. N-fertilized soils did not show the same convergence of molecular ?>composition across ecosystems seen in unfertilized soils (Fig. 3c) likely because of the altered chemistry by the addition of N in the field before the lab incubation. Urea can be hydrolyzed into ammonia and CO_2 by microbial ureases (Mobley and Hausinger, 1989). Nitrification oxidizes ammonium and releases nitrate and H^+. As nitrate is assimilated by plants or microbes into protein, the uncoupled H^+, therefore, acidifies soil (Bolan et al., 1991). Our previous study on the same suite of grassland soils found that N addition led to soil acidification (Zhao et al., 2020), which may facilitate the release of cations (Ca^{2+} or Mg^{2+}) by exchanging cations adsorbing to mineral surfaces with H^+. Cations play bridging roles that bind hydrophilic organic molecules to mineral surfaces (Mikutta et al., 2007; Rasmussen et al., 2018; Rowley et al., 2018). A recent study found that the presence of Ca resulted in a 20% increase in the organic C sorption to ferrihydrite (Sowers et al., 2018) and the identification of Fe, Ca, and organic C ternary systems. Although Ca available for cation bridging may be increased initially with N addition, continued N addition has been found to deplete base cations in soils (Keller et al., under review) as nitrate leaching carries away base cations to balance charge. Nevertheless, H^+ that replaces cations on exchange sites and sorbs to mineral surfaces likely reassociates with negatively charged OM moieties by electrostatic interactions. However, the extent to which the N ferritization impacts the depletion of base cations could vary across sites. For instance, alkaline soils containing more base cations may potentially led to more release of organic molecules bonding with cations due to the breaking of cation bridges by the N fertilization, compared to acidic soils. Thus, the reassembled organic molecules by N fertilization maintained the diversity of molecules between samples across sites and did not converge into more similar chemical composition over time (Fig. 3c).

5. Conclusions

Investigating the dynamics of C chemistry and the potential for retaining C in grassland soils is important for grassland productivity and land-atmosphere C exchange. Increased atmospheric N deposition has been impacting microbial processes and geochemistry in terrestrial ecosystems, including grasslands, at the global scale (Gruber and Galloway, 2008). In line with our hypotheses, this study demonstrates that in grassland soils, the decomposition and mineralization of labile organic molecules, such as carbohydrates, proteins, and amino sugars, were lower in soils with higher concentrations of ferrihydrite minerals (physicochemical preservation). In the absence of new C inputs, compounds that were less energetically favorable for microbial decomposition (lignin-like molecules, tannins, and condensed aromatics) resulted in decomposition products that increased the richness of persistent SOM, independent of soil mineralogy (biochemical preservation). Consistent contributions of both physicochemical and biochemical preservation of SOM resulted in a similar molecular composition of persistent SOM across grasslands. In the presence of N amendments, decomposition was inhibited in the incubation, resulting in diminished C mineralization, reduced respiration, and inhibited convergence of SOM composition across grassland soils, compared to control treatments. Together this study provides empirical evidence of specific molecular classes that persisted with two different mechanisms, leading to a predictable SOM accumulation in grassland ecosystems. Our results indicate that the biochemical complexity of organic molecules primarily drives SOM persistence, independent of soil mineralogy, especially in the presence of N fertilization, where shifts in microbial decomposition alter SOM chemistry, with cascading effects on organo-mineral complexes and soil respiration.

CRediT authorship contribution statement

Qian Zhao: Conceptualization, Methodology, Formal analysis, Investigation, Writing – original draft, Visualization, Project administration. **Allison M. Thompson:** Formal analysis, Investigation, Data curation, Writing – review & editing. **Stephen J. Callister:** Conceptualization, Methodology, Validation, Writing – review & editing, Project administration. **Malak M. Tfaily:** Validation, Investigation, Resources, Writing – review & editing. **Sheryl L. Bell:** Investigation, Resources, Writing – review & editing. **Sarah E. Hobbie:** Validation, Writing – review & editing. **Kirsten S. Hofmockel:** Conceptualization, Methodology, Validation, Writing – review & editing, Supervision, Project administration, Funding acquisition.

Declaration of competing interest

The authors declare that they have no known competing financial interests or personal relationships that could have appeared to influence the work reported in this paper.

Acknowledgement

This work was funded by National Science Foundation (NSF) award to K. S. Hofmockel (NSF-DEB-1556418) and FY16 Laboratory Directed Research and Development program at Pacific Northwest National Laboratory, a multiprogram national laboratory operated by Battelle for the U.S. Department of Energy (DOE) (contract DE-AC05-76RL01830). We thank collaborators from the Nutrient Network (http://nutnet.org) providing us soil property data. We also thank lead investigators, Dana M. Blumenthal (USDA-Agricultural Research Service), Cynthia S. Brown (Colorado State University), Scott L. Collins (University of New Mexico), Julia A. Klein (Colorado State University), Johannes M. H. Knops (University of Nebraska) at each site for operations and maintenance. Coordination and data management of Nutrient Network project have been supported by E. T. Borer, S. E. Hobbie, and E. W. Seabloom from the National Science Foundation Research Coordination Network (NSF-DEB-1042132) and Long-Term Ecological Research (NSF-DEB-1234162 to Cedar Creek LTER) programs, and the UMN Institute on the Environment (DG-0001-13). The research was performed at Environmental Molecular Sciences Laboratory (EMSL), a DOE Office of Science User Facility sponsored by the Office of Biological and Environmental Research. We appreciate the help with graphical editing by Nathan Johnson at Pacific Northwest National Laboratory.

Appendix A. Supplementary data

Supplementary data to this article can be found online at https://doi.org/10.1016/j.scitotenv.2021.150514.

References

Angst, G., Mueller, K.E., Nierop, K.G., Simpson, M.J., 2021. Plant-or microbial-derived? A review on the molecular composition of stabilized soil organic matter. Soil Biol. Biochem. 108189.

Austin, A.T., Yahdjian, L., Stark, J.M., Belnap, J., Porporato, A., Norton, U., Ravetta, D.A., Schaeffer, S.M., 2004. Water pulses and biogeochemical cycles in arid and semiarid ecosystems. Oecologia 141 (2), 221–235.

Bahureksa, W., Tfaily, M.M., Boiteau, R.M., Young, R.B., Logan, M.N., McKenna, A.M., Borch, T., 2021. Soil organic matter characterization by fourier transform ion cyclotron resonance mass spectrometry (FTICR MS): a critical review of sample preparation, analysis, and data interpretation. Environ. Sci. Technol. 55 (14), 9637–9656.

Bai, Y., Wu, J., Clark, C.M., Naeem, S., Pan, Q., Huang, J., Zhang, L., Han, X., 2010. Tradeoffs and thresholds in the effects of nitrogen addition on biodiversity and ecosystem functioning: evidence from Inner Mongolia grasslands. Glob. Chang. Biol. 16 (1), 358–372. https://doi.org/10.1111/j.1365-2486.2009.01950.x.

Bolan, N., Hedley, M., White, R., 1991. Processes of soil acidification during nitrogen cycling with emphasis on legume based pastures. Plant Soil 134 (1), 53–63.

Borer, E.T., Harpole, W.S., Adler, P.B., Lind, E.M., Orrock, J.L., Seabloom, E.W., Smith, M.D., 2014. Finding generality in ecology: a model for globally distributed experiments. Methods Ecol. Evol. 5 (1), 65–73.

Breitling, R., Ritchie, S., Goodenowe, D., Stewart, M.L., Barrett, M.P., 2006. Ab initio prediction of metabolic networks using fourier transform mass spectrometry data. Metabolomics 2 (3), 155–164.

Butterly, C.R., Bünemann, E.K., McNeill, A.M., Baldock, J.A., Marschner, P., 2009. Carbon pulses but not phosphorus pulses are related to decreases in microbial biomass during repeated drying and rewetting of soils. Soil Biol. Biochem. 41 (7), 1406–1416.

Chen, J., Xiao, W., Zheng, C., Zhu, B., 2020. Nitrogen addition has contrasting effects on particulate and mineral-associated soil organic carbon in a subtropical forest. Soil Biol. Biochem. 142, 107708.

Conant, R.T., Paustian, K., Elliott, E.T., 2001. Grassland management and conversion into grassland: effects on soil carbon. Ecol. Appl. 11 (2), 343–355.

Cotrufo, M.F., Wallenstein, M.D., Boot, C.M., Denef, K., Paul, E., 2013. The microbial efficiency-matrix stabilization (MEMS) framework integrates plant litter decomposition with soil organic matter stabilization: do labile plant inputs form stable soil organic matter? Glob. Chang. Biol. 19 (4), 988–995.

Coward, E.K., Thompson, A.T., Plante, A.F., 2017. Iron-mediated mineralogical control of organic matter accumulation in tropical soils. Geoderma 306, 206–216.

Datta, R., Kelkar, A., Baraniya, D., Molaei, A., Moulick, A., Meena, R.S., Formanek, P., 2017. Enzymatic degradation of lignin in soil: a review. Sustainability 9 (7), 1163.

Engels, C., Marschner, H., 1995. Plant uptake and utilization of nitrogen. In: Bacon, P.E. (Ed.), Nitrogen Fertilization in the Environment. Marcel Dekker, Inc, New York, NY, USA, pp. 41–81.

Evans, C.D., Goodale, C.L., Caporn, S.J.M., Dise, N.B., Emmett, B.A., Fernandez, I.J., Field, C.D., Findlay, S.E.G., Lovett, G.M., Meesenburg, H., Moldan, F., Sheppard, L.J., 2008. Does elevated nitrogen deposition or ecosystem recovery from acidification drive increased dissolved organic carbon loss from upland soil? A review of evidence from field nitrogen addition experiments. Biogeochemistry 91 (1), 13–35. https://doi.org/10.1007/s10533-008-9256-x.

Fang, K., Qin, S., Chen, L., Zhang, Q., Yang, Y., 2019. Al/Fe mineral controls on soil organic carbon stock across Tibetan alpine grasslands. J. Geophys. Res. Biogeosci. 124 (2), 247–259.

Feng, X., Simpson, A.J., Simpson, M.J., 2005. Chemical and mineralogical controls on humic acid sorption to clay mineral surfaces. Org. Geochem. 36 (11), 1553–1566.

Fog, K., 1988. The effect of added nitrogen on the rate of decomposition of organic matter. Biol. Rev. 63 (3), 433–462.

Garcia-Pausas, J., Paterson, E., 2011. Microbial community abundance and structure are determinants of soil organic matter mineralisation in the presence of labile carbon. Soil Biol. Biochem. 43 (8), 1705–1713.

Gee, G.W., Bauder, J.W., 1986. Particle-size analysis. Methods of Soil Analysis: Part 1 Physical and Mineralogical Methods. 5, pp. 383–411.

Goodell, B., 2003. Brown-rot Fungal Degradation of Wood: Our Evolving View. ACS Publications.

Gruber, N., Galloway, J.N., 2008. An earth-system perspective of the global nitrogen cycle. Nature 451 (7176), 293–296.

Hall, S.J., Silver, W.L., 2013. Iron oxidation stimulates organic matter decomposition in humid tropical forest soils. Glob. Chang. Biol. 19 (9), 2804–2813. https://doi.org/10.1111/gcb.12229.

Halliwell, B., Gutteridge, J.M., 2015. Free Radicals in Biology and Medicine. Oxford University Press, USA.

Halverson, L.J., Jones, T.M., Firestone, M.K., 2000. Release of intracellular solutes by four soil bacteria exposed to dilution stress. Soil Sci. Soc. Am. J. 64 (5), 1630–1637.

Heckman, K., Lawrence, C.R., Harden, J.W., 2018. A sequential selective dissolution method to quantify storage and stability of organic carbon associated with Al and fe hydroxide phases. Geoderma 312, 24–35.

Hobbie, S.E., Eddy, W.C., Buyarski, C.R., Adair, E.C., Ogdahl, M.L., Weisenhorn, P., 2012. Response of decomposing litter and its microbial community to multiple forms of nitrogen enrichment. Ecol. Monogr. 82 (3), 389–405.

Huang, X., Terrer, C., Dijkstra, F.A., Hungate, B.A., Zhang, W., van Groenigen, K.J., 2020a. New soil carbon sequestration with nitrogen enrichment: a meta-analysis. Plant Soil 454 (1), 299–310.

Huang, X., Zhao, Q., Young, R.P., Zhang, X., Walter, E.D., Chen, Y., Nakouzi, E., Taylor, S.D., Loring, J.S., Wang, Z., Hofmockel, K.S., Rosso, K.M., 2020b. Photo-production of reactive oxygen species and degradation of dissolved organic matter by hematite nanoplates functionalized by adsorbed oxalate. Environ. Sci. Nano 7 (8), 2278–2292. https://doi.org/10.1039/D0EN00365D.

Janusz, G., Pawlik, A., Sulej, J., Świderska-Burek, U., Jarosz-Wilkołazka, A., Paszczyński, A., 2017. Lignin degradation: microorganisms, enzymes involved, genomes analysis and evolution. FEMS Microbiol. Rev. 41 (6), 941–962.

Kaiser, K., Guggenberger, G., 2000. The role of DOM sorption to mineral surfaces in the preservation of organic matter in soils. Org. Geochem. 31 (7–8), 711–725.

Keller, A.B., Borer, E.T., Collins, S.L., Delancey, L.C., Fay, P.A., Hofmockel, K.S., Leakey, A.D.B., Mayes, M.A., Seabloom, E.W., Walter, C.A., Wang, Y., Zhao, Q., Hobbie, S.E., 2021. Soil carbon stocks in temperate grasslands differ strongly across sites but are Insensitive to decade-long fertilization under review.

Kim, S., Kramer, R.W., Hatcher, P.G., 2003. Graphical method for analysis of ultrahigh-resolution broadband mass spectra of natural organic matter, the van krevelen diagram. Anal. Chem. 75 (20), 5336–5344.

Kleber, M., 2010. What is recalcitrant soil organic matter? Environ. Chem. 7 (4), 320–332.

Kleber, M., Mikutta, R., Torn, M.S., Jahn, R., 2005. Poorly crystallinemineral phases protect organic matter in acid subsoil horizons. Eur. J. Soil Sci. 56 (6), 717–725.

Kleber, M., Sollins, P., Sutton, R., 2007. A conceptual model of organo-mineral interactions in soils: self-assembly of organic molecular fragments into zonal structures on mineral surfaces. Biogeochemistry 85 (1), 9–24.

Kleber, M., Eusterhues, K., Keiluweit, M., Mikutta, C., Mikutta, R., Nico, P.S., 2015. Mineral–organic associations: formation, properties, and relevance in soil environments. In: Sparks, D.L. (Ed.), Advances in Agronomy. Vol. 130. Elsevier Academic Press Inc, San Diego, CA, pp. 1–140.

Klotzbücher, T., Kaiser, K., Guggenberger, G., Gatzek, C., Kalbitz, K., 2011. A new conceptual model for the fate of lignin in decomposing plant litter. Ecology 92 (5), 1052–1062.

Kögel-Knabner, I., Guggenberger, G., Kleber, M., Kandeler, E., Kalbitz, K., Scheu, S., Eusterhues, K., Leinweber, P., 2008. Organo-mineral associations in temperate soils: integrating biology, mineralogy, and organic matter chemistry. J. Plant Nutr. Soil Sci. 171 (1), 61–82.

Kramer, M.G., Chadwick, O.A., 2018. Climate-driven thresholds in reactive mineral retention of soil carbon at the global scale. Nat. Clim. Chang. 8 (12), 1104–1108.

Lalonde, K., Mucci, A., Ouellet, A., Gélinas, Y., 2012. Preservation of organic matter in sediments promoted by iron. Nature 483, 198–200. https://doi.org/10.1038/nature10855.

LaRowe, D.E., Van Cappellen, P., 2011. Degradation of natural organic matter: a thermodynamic analysis. Geochim. Cosmochim. Acta 75 (8), 2030–2042.

Lavallee, J.M., Soong, J.L., Cotrufo, M.F., 2020. Conceptualizing soil organic matter into particulate and mineral-associated forms to address global change in the 21st century. Glob. Chang. Biol. 26 (1), 261–273.

Leff, J.W., Jones, S.E., Prober, S.M., Barberán, A., Borer, E.T., Firn, J.L., Harpole, S.W., Hobbie, S.E., Hofmockel, K.S., Knops, J.M.H., McCulley, R.L., La Pierre, K., Risch, A.C., Seabloom, E.W., Schütz, M., Steenbock, C., Stevens, C.J., Fierer, N., 2015. Consistent responses of soil microbial communities to elevated nutrient inputs in grasslands across the globe. Proc. Natl. Acad. Sci. 112 (35), 10967–10972. https://doi.org/10.1073/pnas.1508382112.

Lehmann, J., Kleber, M., 2015. The contentious nature of soil organic matter. Nature 528 (7580), 60–68. https://doi.org/10.1038/nature16069.

Liu, L., Greaver, T.L., 2010. A global perspective on belowground carbon dynamics under nitrogen enrichment. Ecol. Lett. 13 (7), 819–828.

Lu, M., Zhou, X., Luo, Y., Yang, Y., Fang, C., Chen, J., Li, B., 2011. Minor stimulation of soil carbon storage by nitrogen addition: a meta-analysis. Agric. Ecosyst. Environ. 140 (1–2), 234–244.

Lützow, M.V., Kögel-Knabner, I., Ekschmitt, K., Matzner, E., Guggenberger, G., Marschner, B., Flessa, H., 2006. Stabilization of organic matter in temperate soils: mechanisms and their relevance under different soil conditions – a review. Eur. J. Soil Sci. 57 (4), 426–445. https://doi.org/10.1111/j.1365-2389.2006.00809.x.

Mikutta, R., Mikutta, C., Kalbitz, K., Scheel, T., Kaiser, K., Jahn, R., 2007. Biodegradation of forest floor organic matter bound to minerals via different binding mechanisms. Geochim. Cosmochim. Acta 71 (10), 2569–2590.

Mobley, H., Hausinger, R., 1989. Microbial ureases: significance, regulation, and molecular characterization. Microbiol. Mol. Biol. Rev. 53 (1), 85–108.

Ramirez, K.S., Craine, J.M., Fierer, N., 2010. Nitrogen fertilization inhibits soil microbial respiration regardless of the form of nitrogen applied. Soil Biol. Biochem. 42 (12), 2336–2338.

Ramirez, K.S., Craine, J.M., Fierer, N., 2012. Consistent effects of nitrogen amendments on soil microbial communities and processes across biomes. Glob. Chang. Biol. 18 (6), 1918–1927.

Rasmussen, C., Heckman, K., Wieder, W.R., Keiluweit, M., Lawrence, C.R., Berhe, A.A., Blankinship, J.C., Crow, S.E., Druhan, J.L., Pries, C.E.H., Marin-Spiotta, E., Plante, A.F., Schädel, C., Schimel, J.P., Sierra, C.A., Thompson, A., Wagai, R., 2018. Beyond clay: towards an improved set of variables for predicting soil organic matter content. Biogeochemistry 137 (3), 297–306. https://doi.org/10.1007/s10533-018-0424-3.

Riggs, C.E., Hobbie, S.E., Bach, E.M., Hofmockel, K.S., Kazanski, C.E., 2015. Nitrogen addition changes grassland soil organic matter decomposition. Biogeochemistry 125 (2), 203–219.

Rousk, J., Brookes, P.C., Bååth, E., 2009. Contrasting soil pH effects on fungal and bacterial growth suggest functional redundancy in carbon mineralization. Appl. Environ. Microbiol. 75 (6), 1589–1596. https://doi.org/10.1128/AEM.02775-08.

Rousk, J., Brookes, P.C., Bååth, E., 2010. The microbial PLFA composition as affected by pH in an arable soil. Soil Biol. Biochem. 42 (3), 516–520.

Rowley, M.C., Grand, S., Verrecchia, É.P., 2018. Calcium-mediated stabilisation of soil organic carbon. Biogeochemistry 137 (1), 27–49.

Schimel, J.P., 2018. Life in dry soils: effects of drought on soil microbial communities and processes. Annu. Rev. Ecol. Evol. Syst. 49, 409–432.

Schimel, J., Schaeffer, S.M., 2012. Microbial control over carbon cycling in soil. Front. Microbiol. 3, 348.

Schmidt, M.W., Torn, M.S., Abiven, S., Dittmar, T., Guggenberger, G., Janssens, I.A., Kleber, M., Kögel-Knabner, I., Lehmann, J., Manning, D.A., Nannipieri, P., Trumbore, S.E., 2011. Persistence of soil organic matter as an ecosystem property. Nature 478, 49–56. https://doi.org/10.1038/nature10386.

Scurlock, J., Hall, D., 1998. The global carbon sink: a grassland perspective. Glob. Chang. Biol. 4 (2), 229–233.

Sinsabaugh, R.L., 2010. Phenol oxidase, peroxidase and organic matter dynamics of soil. Soil Biol. Biochem. 42 (3), 391–404.

Six, J., Conant, R.T., Paul, E.A., Paustian, K., 2002. Stabilization mechanisms of soil organic matter: implications for C-saturation of soils. Plant Soil 241 (2), 155–176.

Sollins, P., Homann, P., Caldwell, B.A., 1996. Stabilization and destabilization of soil organic matter: mechanisms and control. Geoderma 74 (1–2), 65–105.

Sowers, T.D., Stuckey, J.W., Sparks, D.L., 2018. The synergistic effect of calcium on organic carbon sequestration to ferrihydrite. Geochem. Trans. 19 (1), 4.

Tan, W., Wang, G., Huang, C., Gao, R., Xi, B., Zhu, B., 2017. Physico-chemical protection, rather than biochemical composition, governs the responses of soil organic carbon decomposition to nitrogen addition in a temperate agroecosystem. Sci. Total Environ. 598, 282–288.

Tfaily, M.M., Chu, R.K., Tolić, N., Roscioli, K.M., Anderton, C.R., Paša-Tolić, L., Robinson, E.W., Hess, N.J., 2015. Advanced solvent based methods for molecular characterization of soil organic matter by high-resolution mass spectrometry. Anal. Chem. 87 (10), 5206–5215.

Tfaily, M.M., Chu, R.K., Toyoda, J., Tolić, N., Robinson, E.W., Paša-Tolić, L., Hess, N.J., 2017. Sequential extraction protocol for organic matter from soils and sediments using high resolution mass spectrometry. Anal. Chim. Acta 972, 54–61.

Thevenot, M., Dignac, M.-F., Rumpel, C., 2010. Fate of lignins in soils: a review. Soil Biol. Biochem. 42 (8), 1200–1211.

Tiemann, L.K., Billings, S.A., 2011. Changes in variability of soil moisture alter microbial community C and N resource use. Soil Biol. Biochem. 43 (9), 1837–1847.

Torn, M.S., Trumbore, S.E., Chadwick, O.A., Vitousek, P.M., Hendricks, D.M., 1997. Mineral control of soil organic carbon storage and turnover. Nature 389 (6647), 170.

Treseder, K.K., 2008. Nitrogen additions and microbial biomass: a meta-analysis of ecosystem studies. Ecol. Lett. 11 (10), 1111–1120.

Van Gestel, M., Merckx, R., Vlassak, K., 1993. Microbial biomass responses to soil drying and rewetting: the fate of fast- and slow-growing microorganisms in soils from different climates. Soil Biol. Biochem. 25 (1), 109–123. https://doi.org/10.1016/0038-0717(93)90249-B.

Wagai, R., Mayer, L.M., 2007. Sorptive stabilization of organic matter in soils by hydrous iron oxides. Geochim. Cosmochim. Acta 71 (1), 25–35. https://doi.org/10.1016/j.gca.2006.08.047.

Witt, C., Gaunt, J.L., Galicia, C.C., Ottow, J.C., Neue, H.U., 2000. A rapid chloroform-fumigation extraction method for measuring soil microbial biomass carbon and nitrogen in flooded rice soils. Biol. Fertil. Soils 30 (5), 510–519.

Yu, W.H., Li, N., Tong, D.S., Zhou, C.H., Lin, C.X.C., Xu, C.Y., 2013. Adsorption of proteins and nucleic acids on clay minerals and their interactions: a review. Appl. Clay Sci. 80, 443–452.

Yu, G., Xiao, J., Hu, S., Polizzotto, M.L., Zhao, F., McGrath, S.P., Li, H., Ran, W., Shen, Q., 2017. Mineral availability as a key regulator of soil carbon storage. Environ. Sci. Technol. 51 (9), 4960–4969. https://doi.org/10.1021/acs.est.7b00305.

Zhang, C., Niu, D., Hall, S.J., Wen, H., Li, X., Fu, H., Wan, C., Elser, J.J., 2014. Effects of simulated nitrogen deposition on soil respiration components and their temperature sensitivities in a semiarid grassland. Soil Biol. Biochem. 75, 113–123. https://doi.org/10.1016/j.soilbio.2014.04.013.

Zhao, Q., Poulson, S.R., Obrist, D., Sumaila, S., Dynes, J.J., McBeth, J.M., Yang, Y., 2016. Iron-bound organic carbon in forest soils: quantification and characterization. Biogeosciences 13 (16), 4777–4788. https://doi.org/10.5194/bg-13-4777-2016.

Zhao, Q., Callister, S.J., Thompson, A.M., Kukkadapu, R.K., Tfaily, M.M., Bramer, L.M., Qafoku, N.P., Bell, S.L., Hobbie, S.E., Seabloom, E.W., Borer, E.T., Hofmockel, K.S., 2020. Strong mineralogic control of soil organic matter composition in response to nutrient addition across diverse grassland sites. Sci. Total Environ. 137839. https://doi.org/10.1016/j.scitotenv.2020.137839.

Zhou, J., Xue, K., Xie, J., Deng, Y.E., Wu, L., Cheng, X., Fei, S., Deng, S., He, Z., Van Nostrand, J.D., Luo, Y., 2012a. Microbial mediation of carbon-cycle feedbacks to climate warming. Nat. Clim. Chang. 2, 106–110. https://doi.org/10.1038/nclimate1331.

Zhou, X., Zhang, Y., Downing, A., 2012b. Non-linear response of microbial activity across a gradient of nitrogen addition to a soil from the Gurbantunggut Desert, northwestern China. Soil Biol. Biochem. 47, 67–77. https://doi.org/10.1016/j.soilbio.2011.05.012.

Zhou, Z., Wang, C., Zheng, M., Jiang, L., Luo, Y., 2017. Patterns and mechanisms of responses by soil microbial communities to nitrogen addition. Soil Biol. Biochem. 115, 433–441. https://doi.org/10.1016/j.soilbio.2017.09.015.